Fermi National Accelerator Laboratory

FERMILAB-Pub-91/231-E

Inclusive Jet Cross Section in $\overline{p}p$ Collisions at $\sqrt{s}$ = 1.8 TeV

The CDF Collaboration
Fermi National Accelerator Laboratory
P.O. Box 500, Batavia, Illinois 60510

August 1991

* Submitted to *Physical Review Letters.*

Operated by Universities Research Association Inc. under contract with the United States Department of Energy

CDF/PUB/JET/CDFR/1457
FERMILAB-PUB-91/231-E

Inclusive Jet Cross Section in $\bar{p}p$ Collisions at $\sqrt{s} = 1.8$ TeV

F. Abe,[9] D. Amidei,[4] G. Apollinari,[16] M. Atac,[4] P. Auchincloss,[15] A. R. Baden,[6] N. Bacchetta,[11] M. W. Bailey,[14] A. Bamberger,[4,a] B. A. Barnett,[8] A. Barbaro-Galtieri,[10] V. E. Barnes,[14] T. Baumann,[6] F. Bedeschi,[13] S. Behrends,[2] S. Belforte,[13] G. Bellettini,[13] J. Bellinger,[21] J. Bensinger,[2] A. Beretvas,[4] J. P. Berge,[4] S. Bertolucci,[5] S. Bhadra,[7] M. Binkley,[4] R. Blair,[1] C. Blocker,[2] V. Bolognesi,[13] A. W. Booth,[4] C. Boswell,[8] G. Brandenburg,[6] D. Brown,[6] E. Buckley-Geer,[17] H. S. Budd,[15] G. Busetto,[11] A. Byon-Wagner,[4] K. L. Byrum,[21] C. Campagnari,[3] M. Campbell,[3] R. Carey,[6] W. Carithers,[10] D. Carlsmith,[21] J. T. Carroll,[4] R. Cashmore,[4,a] A. Castro,[11] F. Cervelli,[13] K. Chadwick,[4] G. Chiarelli,[5] W. Chinowsky,[10] S. Cihangir,[4] A. G. Clark,[4] D. Connor,[12] M. Contreras,[2] J. Cooper,[4] M. Cordelli,[5] D. Crane,[4] M. Curatolo,[5] C. Day,[4] F. DeJongh,[4] S. Dell'Agnello,[13] M. Dell'Orso,[13] L. Demortier,[2] B. Denby,[4] P. F. Derwent,[3] T. Devlin,[17] D. DiBitonto,[18] R. B. Drucker,[10] J. E. Elias,[4] R. Ely,[10] S. Eno,[3] S. Errede,[7] B. Esposito,[5] B. Flaugher,[4] G. W. Foster,[4] M. Franklin,[6] J. Freeman,[4] H. Frisch,[3] T. Fuess,[4] Y. Fukui,[9] Y. Funayama,[19] A. F. Garfinkel,[14] A. Gauthier,[7] S. Geer,[4] D. W. Gerdes,[3] P. Giannetti,[13] N. Giokaris,[16] P. Giromini,[5] L. Gladney,[12] M. Gold,[10] K. Goulianos,[16] H. Grassmann,[11] C. Grosso-Pilcher,[3] C. Haber,[10] S. R. Hahn,[4] R. Handler,[21] K. Hara,[19] R. M. Harris,[4] J. Hauser,[4] C. Hawk,[17] T. Hessing,[18] R. Hollebeek,[12] P. Hu,[17] B. Hubbard,[10] B. T. Huffman,[14] R. Hughes,[12] P. Hurst,[5] J. Huth,[4] M. Incagli,[13] T. Ino,[19] H. Iso,[19] H. Jensen,[4] C. P. Jessop,[6] R. P. Johnson,[4] U. Joshi,[4] R. W. Kadel,[10] T. Kamon,[18] S. Kanda,[19] D. A. Kardelis,[7] I. Karliner,[7] E. Kearns,[6] L. Keeble,[18] R. Kephart,[4] P. Kesten,[2] R. M. Keup,[7] H. Keutelian,[4] D. Kim,[4] S. Kim,[19] L. Kirsch,[2] K. Kondo,[19] J. Konigsberg,[6] E. Kovacs,[4] S. E. Kuhlmann,[1] E. Kuns,[17] A. T. Laasanen,[14] J. I. Lamoureux,[21]

Submitted to Physical Review Letters, August 5, 1991

S. Leone,[13] W. Li,[1] T. M. Liss,[7] N. Lockyer,[12] C. B. Luchini,[7] P. Lukens,[4] P. Maas,[21] M. Mangano,[13] J. P. Marriner,[4] M. Mariotti,[13] R. Markeloff,[21] L. A. Markosky,[21] R. Mattingly,[2] P. McIntyre,[18] A. Menzione,[13] T. Meyer,[18] S. Mikamo,[9] M. Miller,[3] T. Mimashi,[19] S. Miscetti,[5] M. Mishina,[9] S. Miyashita,[19] Y. Morita,[19] S. Moulding,[2] J. Mueller,[17] A. Mukherjee,[4] L. F. Nakae,[2] I. Nakano,[19] C. Nelson,[4] C. Newman-Holmes,[4] J. S. T. Ng,[6] M. Ninomiya,[19] L. Nodulman,[1] S. Ogawa,[19] R. Paoletti,[13] A. Para,[4] E. Pare,[6] J. Patrick,[4] T. J. Phillips,[6] R. Plunkett,[4] L. Pondrom,[21] J. Proudfoot,[1] G. Punzi,[13] D. Quarrie,[4] K. Ragan,[12] G. Redlinger,[3] J. Rhoades,[21] M. Roach,[20] F. Rimondi,[4,a] L. Ristori,[13] T. Rohaly,[12] A. Roodman,[3] W. K. Sakumoto,[15] A. Sansoni,[5] R. D. Sard,[7] A. Savoy-Navarro,[4] V. Scarpine,[7] P. Schlabach,[7] E. E. Schmidt,[4] M. H. Schub,[14] R. Schwitters,[6] A. Scribano,[13] S. Segler,[4] Y. Seiya,[19] M. Sekiguchi,[19] M. Shapiro,[10] N. M. Shaw,[14] M. Sheaff,[21] M. Shochet,[3] J. Siegrist,[10] P. Sinervo,[12] J. Skarha,[8] K. Sliwa,[20] D. A. Smith,[13] F. D. Snider,[8] L. Song, [12] R. St. Denis,[6] A. Stefanini,[13] G. Sullivan,[3] R. L. Swartz, Jr.,[7] M. Takano,[19] F. Tartarelli,[13] K. Takikawa,[19] S. Tarem,[2] D. Theriot,[4] M. Timko,[18] P. Tipton,[4] S. Tkaczyk,[4] A. Tollestrup,[4] J. Tonnison,[14] W. Trischuk,[6] N. Turini,[13] Y. Tsay,[3] F. Ukegawa,[19] D. Underwood,[1] S. Vejcik, III,[8] R. Vidal,[4] R. G. Wagner,[1] R. L. Wagner,[4] N. Wainer,[4] J. Walsh,[12] T. Watts,[17] R. Webb,[18] C. Wendt,[21] H. Wenzel,[13] W. C. Wester, III,[10] T. Westhusing,[13] S. N. White,[16] A. B. Wicklund,[1] H. H. Williams,[12] B. L. Winer,[15] J. Wyss, [11] A. Yagil,[4] A. Yamashita,[19] K. Yasuoka,[19] G. P. Yeh,[4] J. Yoh,[4] M. Yokoyama,[19] J. C. Yun,[4] A. Zanetti,[13] F. Zetti,[13] S. Zucchelli [4,a]

The CDF Collaboration

[1] *Argonne National Laboratory, Argonne, Illinois 60439*

[2] *Brandeis University, Waltham, Massachusetts 02254*

(3) *University of Chicago, Chicago, Illinois 60637*

(4) *Fermi National Accelerator Laboratory, Batavia, Illinois 60510*

(5) *Laboratori Nazionali di Frascati, Istituto Nazionale di Fisica Nucleare, Frascati, Italy*

(6) *Harvard University, Cambridge, Massachusetts 02138*

(7) *University of Illinois, Urbana, Illinois 61801*

(8) *The Johns Hopkins University, Baltimore, Maryland 21218*

(9) *National Laboratory for High Energy Physics (KEK), Japan*

(10) *Lawrence Berkeley Laboratory, Berkeley, California 94720*

(11) *Universita di Padova, Instituto Nazionale di Fisica Nucleare, Sezione di Padova, I-35131 Padova, Italy*

(12) *University of Pennsylvania, Philadelphia, Pennsylvania 19104*

(13) *Istituto Nazionale di Fisica Nucleare, University and Scuola Normale Superiore of Pisa, I-56100 Pisa, Italy*

(14) *Purdue University, West Lafayette, Indiana 47907*

(15) *University of Rochester, Rochester, New York 14627*

(16) *Rockefeller University, New York, New York 10021*

(17) *Rutgers University, Piscataway, New Jersey 08854*

(18) *Texas A&M University, College Station, Texas 77843*

(19) *University of Tsukuba, Tsukuba, Ibaraki 305, Japan*

(20) *Tufts University, Medford, Massachusetts 02155*

(21) *University of Wisconsin, Madison, Wisconsin 53706*

Abstract

We present a measurement of the inclusive jet cross section in $\bar{p}p$ collisions at $\sqrt{s} = 1.8$ TeV at the Fermilab Tevatron using the Collider Detector at Fermilab (CDF). Good agreement is seen with the predictions of recent next-to-leading ($\mathcal{O}(\alpha_s^3)$) predictions. The dependence of the cross section on clustering size is measured. An improved limit on Λ_c, a term characterizing possible quark substructure, is set at 1.4 TeV (95 % CL).

.....

Recently, calculations of the inclusive jet cross section, $\sigma(\bar{p}p \rightarrow \text{Jet} + X)$, have become available at next-to-leading order ($\mathcal{O}(\alpha_s^3)$)[1,2,3]. The new QCD predictions explicitly include jet definitions at the parton level which can be directly related to experimental jet algorithms. This property allows a comparison of the jet cross section to theory for different effective jet sizes and is not a feature of the leading order ($\mathcal{O}(\alpha_s^2)$) calculation. In addition, the reduction of both experimental and theoretical uncertainties have improved the precision of the comparison of data to QCD. A data sample of 4.2 pb^{-1} from an extended run of the Fermilab Tevatron $\bar{p}p$ Collider has given a measurement of the inclusive jet cross section over 7 orders of magnitude, from 35 to 450 GeV in transverse energy. The increased data set has also allowed an increased sensitivity to the presence of possible quark substructure.

The CDF detector has been described in detail elsewhere [4]. The detector elements most relevant to this study are the central calorimeters, which cover the

pseudorapidity range $|\eta| \leq 1.1$ ($\eta \equiv -ln\,tan(\theta/2)$ and θ is the polar angle with respect to the beam). These calorimeters are segmented into projective towers of $\Delta\eta \times \Delta\phi = 0.1 \times 15^o$. The detector was triggered on the presence of a localized cluster of energy in the calorimeter [7]. In order to span a large range of cross sections, three separate thresholds were imposed on the transverse energy, E_t, of the trigger clusters of 20, 40, and 60 GeV. The 20 and 40 GeV triggers were prescaled to accept 1 in 300 and 1 in 30 events, respectively.

Jets were identified using a cone algorithm, described fully in [7], based on the measured event vertex as the origin. Contiguous seed towers with $E_t > 1$ GeV were selected to form preclusters. Using the E_t weighted centroid of preclusters as a starting point, jet clusters were formed by including all towers with $E_t > 100$ MeV inside a cone of radius R $= \sqrt{(\Delta\eta)^2 + (\Delta\phi)^2}$. A tower is included in a cluster if its center is inside the cone, otherwise it is excluded. If a cluster shared more than 75 % of its energy with a cluster of higher energy, the two were merged together, otherwise, they were defined as separate, and towers common to both clusters were assigned to the jet with the nearest centroid. Jet energy, E, was determined using a scalar sum of tower energies in the cone. E_t was taken as E $\sin\theta$, where θ was taken from the angle between a line drawn from the cluster center to the event vertex position and the beamline. The above algorithm is very similar to the jet definition employed at the parton level in producing the $\mathcal{O}(\alpha_s^3)$ predictions for comparison [3]. The jets were clustered using 3 different radii, R = 0.4, 0.7, and 1.0, to examine the R dependence.

A set of cuts was placed on the data to ensure uniform acceptance. The event vertex was required to be within 60 cm of the center of the detector along the beamline.

In order to ensure a triggering efficiency for clusters greater than 98 %, thresholds were placed on the minimum offline cluster E_t for each trigger. These were 35, 60 and 100 GeV for the 20, 40 and 60 GeV triggers respectively. These cuts were based on the offline cluster efficiency determined in the region of E_t where the data from different triggers overlapped. Backgrounds from cosmic ray bremsstrahlung were rejected with better than 99.5% efficiency using criteria nearly identical to those described in reference [6]. Finally, jets in the sample were required to have $0.1 \leq |\eta| \leq 0.7$ to ensure uniform detector response and good containment in the central detector.

The measured jet E_t spectrum is distorted due to several effects. First, the low energy response of the calorimeter to single hadrons is nonlinear, but is linear for photons and electrons. The jet energy measured in the calorimeter is a convolution of the single particle response with the jet fragmentation spectrum. This, when combined with energy losses in uninstrumented regions, can give rise to a mean response that is typically less than the true jet energy. Secondly, the effect of the broad jet energy resolution on a steeply falling spectrum distorts the measured spectrum. The RMS resolution for jets in the range $35 \leq E_t \leq 200$ GeV can be approximated by $\sigma_{rms} = 0.1E_t + 1$ GeV. Finally, the underlying event not associated with the hard scattering process can contribute energy into the clustering cone which should not be included in the jet energy. The average E_t density (uncorrected for nonlinearities) from the underlying event was measured in regions of the calorimeter far from jet clusters and was approximately 1.2 ± 0.3 GeV per unit area in the $\eta - \phi$ plane. No energy corrections were applied for energy falling outside of the clustering cone, as

this, in principle, should be taken into account by the next-to-leading order calculations [2,3,8].

The effects of resolution smearing and loss of energy associated with calorimeter nonlinearity, were determined and corrected using the following procedure. The response of the calorimeter to hadrons between 0.5 and 250 GeV was determined from test beam data and isolated tracks in the central tracking chamber. The fragmentation spectrum was also measured using the charged particle [9]. A detector simulation incorporated the response of the calorimeter to single hadrons, including the effects of variable response across the face of towers. This simulation was combined with an event generator which used a Field-Feynman [10,11] fragmentation scheme tuned to reproduce the jet data. The response of the detector to jets was parameterized for the E_t range 10 to 500 GeV, and, in conjunction with the raw jet spectrum, was used to determine an unfolded jet E_t spectrum. This procedure corrected for all effects described above and was performed separately for each clustering radius, R.

We assign systematic uncertainties to the data based on our knowledge of detector effects and jet fragmentation. The largest uncertainties come from the modeling of the calorimeter response [12]. Because of the steeply falling E_t spectrum a small error in energy scale can generate large uncertainties in the cross section. For values of jet E_t above 80 GeV, the uncertainty on the cross section is typically 22 % and is independent of E_t. Below 80 GeV, the uncertainty rises as high as 60 %. These uncertainties are smaller than those reported in previous measurements of the jet cross section [6,13].

The cross section for a clustering radius R=0.7 is shown in figure 1 along with

a prediction from next-to-leading order QCD [3] using the HMRS set B [14] parton distribution functions, with the renormalization scale choice $\mu = E_t$. The data are presented as an average over the pseudorapadity interval $0.1 \leq |\eta| \leq 0.7$, and are shown in table 1. The predictions and the data show good agreement over 7 orders of magnitude of cross section and E_t ranging from 35 to 450 GeV. In figure 2 the ratio of (data - theory)/theory is plotted to show the level of agreement on a linear scale. The $\mathcal{O}(\alpha_s^3)$ calculation using the HMRS set B parton distribution function serves as a reference (*i.e.* is zero in figure 2). To illustrate the variation associated with different parton distribution functions, we have also shown curves derived from other sets [14,16]. All normalizations in figures 1 and 2 are absolute. E_t dependent systematic uncertainties are included in error bars; the E_t independent uncertainty is indicated in figure 2 as the horizontal dotted lines. The E_t dependent systematic uncertainties, which dominate at $E_t \leq 150$ GeV, are highly correlated from point to point. For R=0.7, the $\mathcal{O}(\alpha_s^3)$ cross sections have a theoretical uncertainty associated with higher order diagrams which have not been calculated. This uncertainty is estimated from the sensitivity to the choice of renormalization scale, μ, which is used for evaluating the strong coupling constant $\alpha_s(\mu)$ and for the evolution of the parton distribution functions. The scale, μ, was varied between $E_t/4 \leq \mu \leq E_t$, and gives a cross section variation of ≈ 10 %, which is substantially smaller than the corresponding uncertainty (≈ 50 %) for the leading order $\mathcal{O}(\alpha_s^2)$ calculation [17].

We have made a quantitative comparison of the data to the $\mathcal{O}(\alpha_s^3)$ predictions using four recent parton distribution function sets (HMRS sets B and E; MT sets B and S) [14,16], by normalizing the theory to the data. This is done by minimizing a χ^2

which takes into account systematic uncertainties and correlations from point-to-point and was performed for $E_t \geq 80$ GeV to minimize systematic uncertainties associated with the E_t scale. The normalization constants were 1.15, 1.13, 1.27 and 1.29 for HMRS sets B,E, MTS sets S and B respectively. The deviation of the normalizations from unity is of the same magnitude as the uncertainty (≈ 20 %) on the cross section. We can then use the resulting χ^2 values to determine how well the shape of the theoretical predictions agree with the data. The confidence levels associated with these were 19 %, 0.1 %, 49 % and 56 % respectively for the above sets of parton distribution functions and 30 degrees of freedom. HMRS set B, MT sets S and B give acceptable fits, and the shape of HMRS set E is inconsistent, mostly in the region between 80 and 250 GeV.

The variation of the jet cross section as a function of clustering radius, R, is shown in figure 3 for jets of 100 GeV E_t, along with $\mathcal{O}(\alpha_s^3)$ predictions (MRSB [15] parton distribution functions) with three different choices of renormalization scale, μ. Only statistical errors have been plotted with the data. The curves represent the typical theoretical uncertainty on the R dependence of the cross section and exhibit a smaller uncertainty near R=0.7 than for other values of R. We fit the data to the function $A + B\,ln\,R$ where A and B are free parameters [8]. The result of the fit is $A = 0.79 \pm 0.02$ nb/GeV and $B = 0.49 \pm 0.03$ nb/GeV. The derivative of this function with respect to R, evaluated at R=0.7 is 0.70$\pm$0.05 nb/GeV, compares favorably to an $\mathcal{O}(\alpha_s^3)$ prediction of 0.5$\pm$0.2 nb/GeV [18,19].

The presence of quark substructure can appear as an enhancement of the cross section at high E_t. This effect is conventionally parameterized in terms of a 4-Fermi

interaction of unit strength between left handed quarks, characterized by the constant Λ_c with units of energy [20]. In order to search for quark substructure, predictions for the inclusive E_t spectrum for different parton distribution functions and values of Λ_c have been compared to the data. Only leading order ($\mathcal{O}(\alpha_s^2)$) calculations that include this contact term are available at present. Because of this, we have fit the data using a cone of $R = 1.0$ to minimize the effects of energy outside of the cone. The fits are performed by normalizing the predictions to the data using an overall multiplicative factor in the region $80 \leq E_t \leq 160$ GeV, where contributions from the contact term for $\Lambda_c \geq 750$ GeV are negligible. The fitted curves are then extrapolated to the region $E_t \geq 160$ GeV where they are compared to the data. The comparison with data takes into account Poisson statistics for bins with a small number of entries, and also the correlations associated with systematic uncertainties. We have used only recent sets of structure functions for this test (HMRS sets B and E, MT sets S, B) [14,16]. The set HMRS set E was excluded due to poor fits in the normalization region. A lower limit of 1.4 TeV is set on Λ_c at the 95 % confidence level. This represents the most conservative limit from the above structure functions (HMRS set B). The largest contribution to the χ^2 in this limit comes from the region $200 \leq E_t \leq 300$ and the absence of events above 420 GeV. The Compton wavelength, $\lambda = \hbar/\Lambda_c c$, associated with this limit is 1.4×10^{-4} Fm.

To summarize, we have measured the inclusive jet cross section in $\bar{p}p$ collisions at $\sqrt{s} = 1.8$ TeV. The data span 7 orders of magnitude in cross section, and include the highest values of E_t measured to date, allowing a stringent test of both higher order QCD and possible quark substructure. Next-to-leading order QCD calculations give

a reasonable description of the data. The variation of jet cross section with clustering radius, R, is consistent with a next-to-leading order ($\mathcal{O}(\alpha_s^3)$) calculation [3]. Finally a search for possible quark substructure has given a lower limit of 1.4 TeV (95 % CL) on the compositeness energy scale Λ_c.

We thank the Fermilab accelerator division and the technical staffs of the participating institutions for their invaluable contributions. This work is supported in part by the U.S. Department of Energy and National Science Foundation, the Italian Istituto Nazionale di Fisica Nucleare, the Ministry of Science, Culture and Education of Japan, and the Alfred P. Sloan Foundation. We also wish to thank S. Ellis, M. Greco, P. Guillet, Z. Kunszt and D. Soper for useful discussions and for providing results of their calculations.

References

[1] R. Ellis and J. Sexton, Nucl. Phys. **B 269** 445 (1986).

[2] F. Aversa *et al.* , Phys. Lett. **B210** , 225 (1988).

[3] S. Ellis, Z. Kunszt and D. Soper, Phys. Rev. Lett., **62** 2188 (1989); Phys. Rev. Lett. **64** 2121 (1990).

[4] F. Abe *et al.* (CDF collaboration), Nucl. Instr. Meth. A **271**, 387 (1988).

[5] D. Amidei *et al* , Nucl. Instr. Meth. A **269**, 260 (1988).

[6] F. Abe *et al.* (CDF collaboration), Phys. Rev. Lett **62**, 613 (1989).

[7] F. Abe *et al.* , Fermilab Preprint FNAL PUB 91/181, submitted to Phys. Rev. D. (1991).

[8] S. Ellis, talk presented at Snowmass 1990 High Energy Physics Workshop, Research Directions for the Decade", DOE preprint DOE/ER/4043-27 (1991).

[9] F. Abe *et al.* , Phys. Rev. Lett. **65** , 968 (1990).

[10] R. Field and R. Feynman, Nucl. Phys. **B136,** 1 (1978).

[11] F. Paige and S. Protopopescu, BNL-38034 (1986); and in Proceedings of the 1986 Summer Study on the Physics of the Superconducting Supercollider, Donaldson, R. and Marx, J. ed, 320 (1986).

[12] J. Huth, in *Proceedings of the Workshop on Calorimetry for the SSC, Tuscaloosa Alabama, 1989,* edited by R. Donaldson, G. Gilchriese (World Scientific, Singapore 1990).

[13] J. Alitti *et al.* (UA2 Collaboration) CERN Preprint CERN-PPE/90-188 (1990), submitted to Phys. Lett.

[14] P. Harriman, A. Martin, R. Roberts and W. Stirling, Rutherford Laboratory Preprint RAL-90-007 (1990).

[15] A. Martin, R. Roberts and W. Stirling, Phys. Rev. D **37** 1161 (1988).

[16] J. Morfin and W.K. Tung, Fermilab Preprint Fermilab-Pub-90/74 (1990).

[17] S. Ellis, Z. Kunszt, D. Soper, Proceedings of the 1990 Meeting of the Division of Particles and Fields of the American Physical Society, Houston Texas, 3-6 Jan 1990, edited by W. Bonner and H. Miettinen, World Scientific Singapore p. 603 (1990).

[18] S. Ellis, Z. Kunszt, and D. Soper, private communication (1991).

[19] This issue has also been discussed in: F. Aversa, *et al* , Z. Phys. **C49** 459 (1991).

[20] E. Eichten, K. Lane, and M. Peskin, Phys. Rev. Lett., **50** , 811, (1983).

Table 1: Jet cross section for a jet clustering cone size of 0.7. Systematic uncertainties have a large degree of correlation from bin to bin.

Mean E_t (GeV)	Cross Section	± Statistical	± Systematic (nb/GeV)
10.06	75800	±2030	+53700 − 68300
14.99	11400	±783	+6640 − 9080
21.82	2400	±307	+935 − 1330
28.71	279	+128 − 91	+218 − 310
35.48	188	±7.53	+67 − 95.4
41.63	77.4	±1.08	+27.5 − 37.7
47.61	37.1	±0.715	+12.8 − 16.8
53.54	20.1	±0.520	+6.41 − 8.01
59.93	10.5	±0.373	+3.26 − 3.80
66.23	6.27	±0.286	+1.77 − 1.89
72.29	3.77	±0.0679	+1.03 − 0.999
78.15	2.49	±0.0550	+0.652 − 0.563
83.81	1.79	±0.0467	+0.434 − 0.357
89.31	1.17	±0.0378	+0.298 − 0.245
94.82	0.818	±0.0318	+0.208 − 0.171
100.19	0.574	±0.0267	+0.149 − 0.122
105.60	0.427	±0.0231	+0.107 − 0.0884
111.04	0.321	±0.0200	+0.0783 − 0.0645
116.44	0.219	±0.00312	+0.0579 − 0.0477
121.76	0.166	±0.00272	+0.0434 − 0.0357
127.12	0.122	±0.00233	+0.0328 − 0.0270
132.49	0.0926	±0.00204	+0.0249 − 0.0205

Table 1 continued...

Mean E_t (GeV)	Cross Section	± Statistical		± Systematic (nb/GeV)	
137.77	0.0712	±0.00179		+0.0192	− 0.0158
143.05	0.0552	±0.00158		+0.0149	− 0.0122
148.48	0.0440	±0.00141		+0.0115	− 0.00948
153.71	0.0344	±0.00125		+0.00905	− 0.00745
158.93	0.0283	±0.00114		+0.00716	− 0.00589
164.25	0.0219	±0.00100		+0.00567	− 0.00467
171.89	0.0165	±0.000618		+0.00408	− 0.00336
182.20	0.0111	±0.000508		+0.00266	− 0.00219
193.04	0.00656	±0.000392		+0.00173	− 0.00142
203.47	0.00368	±0.000294		+0.00116	− 0.000952
215.73	0.00256	±0.000202		+0.000733	− 0.000604
231.88	0.00157	±0.000159		+0.000412	− 0.000339
246.86	0.000902	±0.000121		+0.000247	− 0.000203
264.86	0.000470	±0.0000872		+0.000137	− 0.000113
281.96	0.000381	±0.0000685		+0.0000801	− 0.0000659
302.22	0.000198	+0.0000630	− 0.0000490	+0.0000436	− 0.0000359
322.87	0.0000867	+0.0000468	− 0.0000321	+0.0000241	− 0.0000198
343.88	0.0000621	+0.0000422	− 0.0000269	+0.0000135	− 0.0000111
380.72	0.0000252	+0.0000246	− 0.0000137	+0.00000523	− 0.00000431
418.55	0.0000104	+0.0000137	− 0.00000671	+0.00000213	− 0.00000175

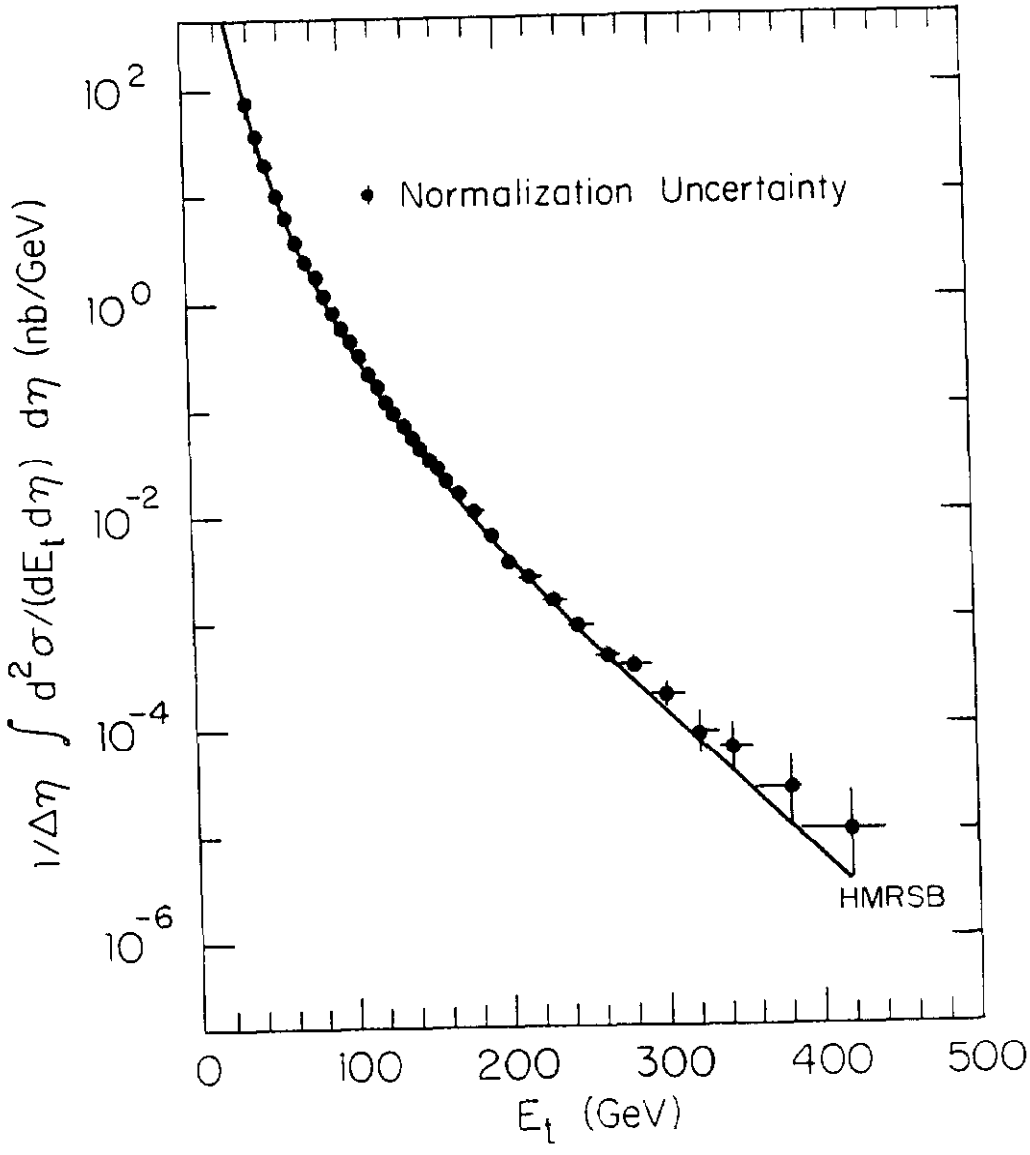

Figure 1: Inclusive E_t spectrum for a cone size of $R = 0.7$, averaged over the pseudorapidity interval $0.1 \leq |\eta| \leq 0.7$. The curve represents the predictions of a next-to-leading order QCD calculation by S. Ellis *et al* [3]. The error bars on the data represent statistical and E_t dependent systematic errors. An overall normalization uncertainty is also indicated.

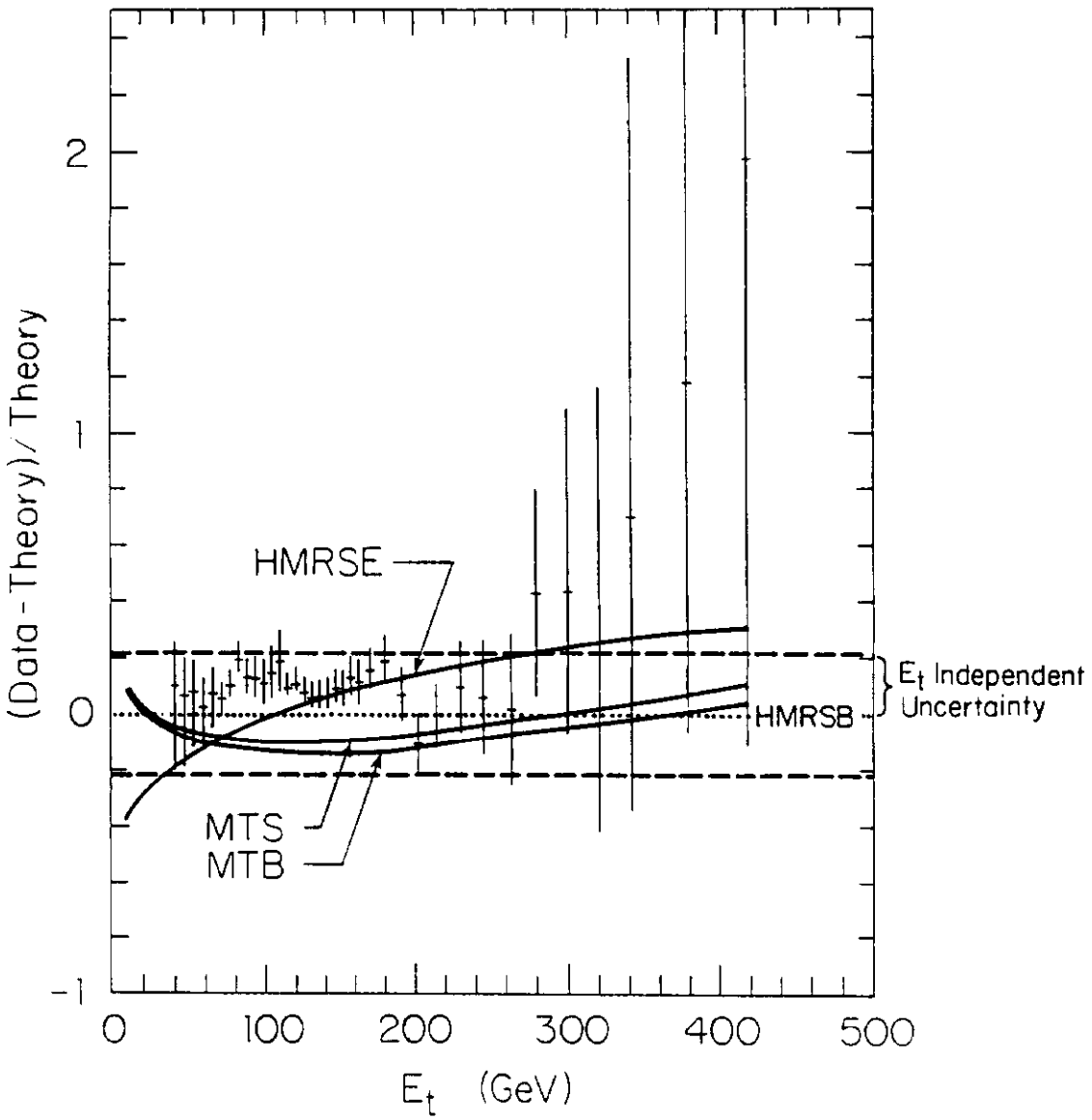

Figure 2: The inclusive jet E_t spectrum compared to theory as the ratio of (data-theory)/theory. The horizontal dashed lines indicate the E_t independent systematic uncertainty on the data, while the error bars include the E_t dependent part. The $\mathcal{O}(\alpha_s^3)$ prediction using the HMRS set B [14] structure function set is used as a reference. The predictions using other sets of structure functions are also shown.

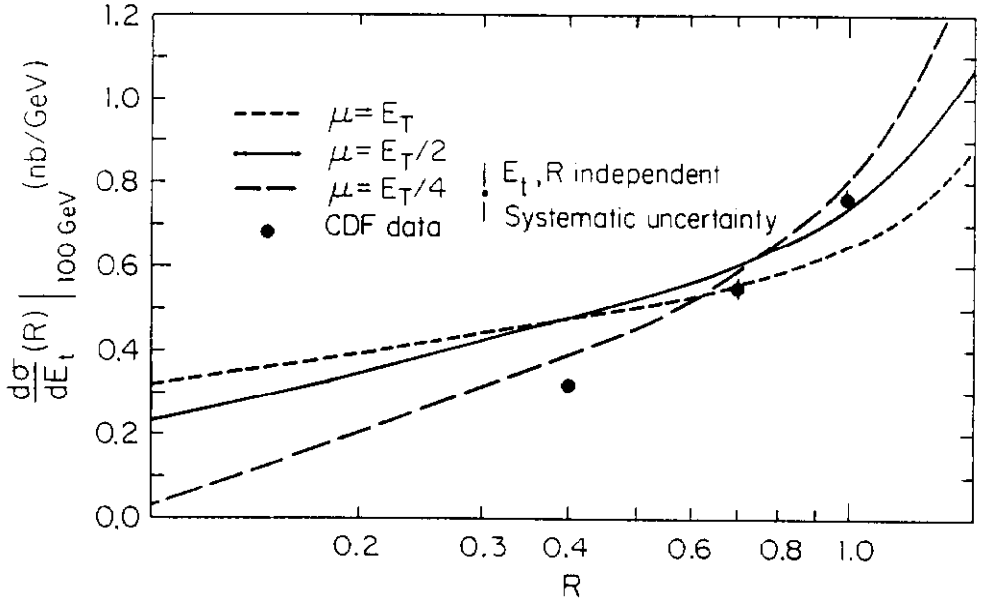

Figure 3: The variation of jet cross section with clustering cone size, R, for jets of 100 GeV E_t. Statistical errors only are plotted on the data points. An overall, R independent, systematic uncertainty is also indicated. The curves represent a range of theoretical predictions associated with different choices of renormalization scale, μ, using the MRSB [15] parton distribution function.